PCCP

Interaction between probe molecules and zeolites.

Part II:†Interpretation of the IR spectra of CO and N_2 adsorbed in NaY and NaRbY

A. V. Larin,[a] D. P. Vercauteren,*[b] C. Lamberti,[c] S. Bordiga[c] and A. Zecchina[c]

[a] *Laboratory of Molecular Beams, Department of Chemistry, Moscow State University, Leninskie Gory, Moscow, B-234, 119899, Russia*
[b] *Institute for Studies in Interface Sciences, Laboratoire de Physico-Chimie Informatique, Facultés Universitaires Notre Dame de la Paix, Rue de Bruxelles 61, B-5000 Namur, Belgium*
[c] *Dipartimento di Chimica Fisica, Chimica Inorganica e Chimica dei Materiali, via P. Giuria 7, 10125 Torino, Italy*

Received 9th August 2001, Accepted 29th January 2002
First published as an Advance Article on the web 29th April 2002

The interaction energy and band shift values of the fundamental vibrational modes of CO and N_2 adsorbed within the NaY and NaRbY zeolite forms are calculated using a pair-wise addition scheme. A clear difference between the most stable positions of CO and N_2 in NaY and NaRbY is observed. While, for NaY, both diatomic probes are close to the alkali-metal ion, this is not the case for NaRbY. For CO, the isolated Rb^+–CO pair-wise interaction cannot describe the system, because the Rb–CO and O–CO distances are comparable whereas for N_2 within NaRbY, the molecule is closer to the framework oxygens than to the Rb. The influence of both molecular and zeolite framework parameters (ionic charges, polarizabilities, and radius) on the interaction energy and band shift values is definitively proven.

I. Introduction

Zeolites are crystalline aluminosilicates whose applications in the areas of chemical synthesis and separation processes are continually increasing. Therefore, IR studies of small probe molecules like carbon monoxide, nitrogen, and hydrogen adsorbed within zeolite frameworks have become a popular and powerful method for understanding the adsorbed state of the guest molecule and the host system. At the same time, numerous theoretical attempts[1] have helped to provide a deeper insight into the influence of the zeolite structure on the spectra of the adsorbed molecules. For example, for CO, the band shift (BS) of the fundamental vibrational transition of adsorbed CO has been correlated not only to the type of cation directly involved in the adsorption process[1] but also to the electrostatic influence of the framework. In relation to this, it is worth recalling that appreciable variations of the BS values for adsorbed H_2[2,3] and CO[3] within the sodium exchanged form of different zeolites (ZSM-5, MOR, X, Y, A) have indicated a strong influence on the interaction energy (IE) of the whole zeolite framework. These findings indicate that the total BS cannot be interpreted only on the basis of the isolated Me^+–CO pair approach (Me = Li, Na, K, Rb, Cs).[4] For example, the framework influence on the adsorption of methane was partially mimicked by constructing a cluster around the cation, *i.e.*, $Me[HAl(OH)_3]$.[5,6] Similarly, the BS values of CO adsorbed within ZSM-5 and the main channel sites of mordenite (MOR)[7] have been interpreted on the basis of a simple model including only the electrostatic field induced by Me^+, the two closest oxygen atoms, and an additional field component generated by the remaining zeolite framework polarized by the presence of the cation, but neglecting the effects of the adjacent cations. This crude approximation is acceptable for low cation populated zeolites only (*e.g.*, ZSM-5 or the main channel sites of MOR) but cannot be extended to frameworks with lower Si/Al ratios such as zeolites Y, X or A. This trend in the development of models[4–7] clearly underlines the necessity of treating, as accurately as possible, the IE between the probe and zeolite structure represented *via* a more general spatial model including explicitly the influence of all the framework and extraframework atoms.

This approach is even more necessary if the influence of the cationic nature of Y type zeolites on their activity is considered, as has been already demonstrated for the aldol condensation reaction of acetone,[8] the disproportionation of alkylsilanes,[9] *etc*. On this basis, it is evident that variation of the cation location can change strongly both the ratio between the IE components and the total IE value. Theoretical investigations are thus necessary to clarify the influence of this ratio on the reaction mechanisms. They surely will help in the experimental assignments of the cation positions proposed for the Zn,[10] Cd,[11,12] La,[13,14] Cu,[15] Rb,[16] and other forms of Y zeolite. In our previous study,[16] IR spectra of CO and N_2 probes in the adsorbed state were also recorded.

Calculations of the probe position inside a zeolite should take into account all components of the IE, *e.g.*, electrostatic, inductive, dispersive, charge transfer, exchange-overlap or repulsive.[17] Similarly, the effect of all contributions to the BS value coming from the different IE components should be considered. This is possible using either *ab initio* approaches or through simplified pair-wise addition schemes. The second method does not allow us to estimate the charge transfer contribution, but this drawback is of minor importance (this is practically true when dealing with alkali-metal cations). The

† For part I see ref. 19.

 DOI: 10.1039/b107242k

small magnitude of the charge transfer has indeed been demonstrated by energy decomposition procedures like the constrained space orbital variation (CSOV).[1,18]

In this work, we will use the pair-wise addition scheme to evaluate the IE and BS. The BS values can be computed provided that the dependences of all multipole moments and polarizabilities of the probe molecule, as well as the dispersive and repulsive coefficients for all "host–guest" atom pairs are known with respect to the probe internuclear distance ρ. Within the pair-wise scheme, it has been shown that the ρ dependence of the repulsive coefficients can be determined from the routine condition of the equilibrium position of the adsorbed molecule relative to all ions of the adsorbent. If such an equilibrium does not exist for the O_{zeol}–CO pair (owing to the negative charge on C), a possible approximation of the repulsive coefficients with ρ could be achieved allowing a stable O_{zeol}–CO configuration for the higher vibrational states of CO within the Na_4Ca_4A zeolite.[19]

Therefore, we have calculated the IE and BS values for CO and N_2 adsorbed within the Na and Rb forms of Y zeolite in the same way as for Na_4Ca_4A.[19] As all theoretical bases as well as all necessary CO and N_2 molecular properties are presented in the preceding paper,[19] we start with the ionicity determination for the Y model and with an additional intercombination rule for the dispersive coefficients used in this paper as compared to ref. 19. In section III, we will illustrate the main characteristics of the zeolite models. In section IV, all results for the CO/NaY and CO/NaRbY models based on the comparison between the calculated and experimental BS values will be discussed. In section V, we will present the problem of the BS calculations for the N_2 case within the various chosen zeolite models. Finally, a comparison of the electrostatic field values with available experimental estimations is made in section VI.

II. Ionicity of Y zeolite models and intercombination rules

The total interaction energy (IE) U_{tot} between the adsorbed molecule and the zeolite framework can be evaluated as the sum of the electrostatic U_{elec}, inductive U_{ind}, dispersive U_{disp}, and repulsive U_{rep} interaction contributions. All necessary expressions are given in detail in ref. 19.

The total charge of each cationic (or anionic) zeolite subunit has been determined through the ionicity parameter q_0.[20] For zeolite Y with Si/Al = 3, corresponding to the total formula $NaSi_3AlO_8$[21] the relation is:

$$q_0 = q(\mathrm{Na}) + 3q(\mathrm{Si}) + q(\mathrm{Al}) = \sum_{k=1}^{8} |q(\mathrm{O}_k)| \qquad (1)$$

It is worth mentioning that such q_0 computation leads to a larger ionicity by a factor of 2 as compared to the value used for the A type zeolites.[19,20]

The charge dependences of the ionic polarizabilities and radius (Table 1 for Rb and Table 3 in ref. 19 for Na, O, Si, and Al) require the consideration of all framework atoms in all interaction terms. As has been widely shown,[25] the neglect of a part of the electrons for example related to the framework Al or Si atoms provides zeolite models with different electron redistributions at different q_0. Such a difference obviously leads to errors in the dispersive term which vary with the ionicity. This is particularly important because of the intercombination rule for the van der Waals (vdW) coefficients C_{ij}. A common expression can be used on the basis of both the Kirkwood–Müller (KM) and Slater–Kirkwood (SK) rules. If we express the diamagnetic susceptibility *via* α_i and n_i,[26] *e.g.*, in atomic units: $\chi_i = \sqrt{n_i \alpha_i}/(4c^2)$, c being the velocity of light, then the C_{ij} values can be given by:

$$C_{ij} = 3/2\ \alpha_i \alpha j / [(\alpha_i/n_i)^{1/2} + (\alpha_j/n_{AB})^{1/2}] \qquad (2)$$

where α_i and n_i are the static polarizability and number of electrons of the framework ion i, α_j and n_{AB} are the static polarizability and number of electrons of the AB diatomic probe (j corresponding to the parallel and perpendicular ion–molecule orientations without difference between the i–AB and i–BA geometries). In formula (2), the number of electrons is calculated as $n_i = n_{0i} - q(i)$, n_{0i} being the electron number of the respective ion i. For the KM case, n_{0i} is the total number of electrons, *i.e.*, $n_{CO} = n_{N2} = 14$, while for the SK rule, n_{0i} is the number of valence electrons, *i.e.*, $n_{CO} = n_{N2} = 10$.

Table 1 Polarizability α and radius r functions expressed as linear $X(q) = X(0) - Aq$ forms (a_0^3 and a_0) for Rb (see ref. 19 for Na, O, Si, and Al)

$X(q)$	q-Dependence	$X(0)$	A
α	Linear	43.9[a]	42.2[b]
R	Linear	2.48[c]	1.814[d]

[a] Ref. 22. [b] Estimated A value considering $\alpha(Rb^+) = 1.7\ a_0^{3}$[22] ($a_0^3 = 0.148 \times 10^{-30}$ m^3). [c] Ref. 23. [d] Estimated A value considering $r(Rb^+) = 1.52\ a_0$[24] ($a_0 = 0.5292 \times 10^{-10}$ m).

III. Zeolite Y models

We considered all 156 framework atoms[21] belonging to the central unit cell of NaY with the lattice constant ($a = b = c$) of 24.767 Å and the $F23$ spatial group. For N_2 interacting with NaY, we here show that a fragment containing 19 cells is large enough to give accurate IE and BS values. For the NaRbY form, we have assumed that all atoms have the same coordinates as in NaY, the Rb substituting Na at position II within the supercage.[21] The four Na_I ions within the hexagonal prisms are assumed to remain in their positions. The same charge ratio $q(\mathrm{Al})/q(\mathrm{Si}) = 0.8447$[21] was used for all zeolite models considered below.

Two different O atom types are present in NaY or NaRbY, *i.e.*, those belonging to the Si–O–Si moieties (crystallographically independent O_2, O_4, O_5, O_7 atoms, see Table 7 of ref. 27) and those of the Si–O–Al (O_1, O_3, O_6, O_8) ones. Even though the O atoms of each type of Si–O–T moiety (T = Si or Al) in zeolite Y have very similar average T–O bond distances (R) and Si–O–T angles (ϑ) (which together determine the O charge value[27]) within each of the two groups, they will be considered as separate ones. For Si–O–Si, our results based on the ps-21G*(Si)/6-21G*(O) basis set periodic Hartree–Fock (PHF) computations[28] showed that the charge ratios $q(O_4)/q(O_i)$ are 1.003, 1.003, and 1.004, for i = 7, 5, 2, respectively. One should mention that this level of basis set corresponds to nearly "convergent" atomic charges in the series STO-3G → 88-51G(Si)/6-21G(O) → ps-21G*(Si)/6-21G(O) → 6-21G*(Si, O) for all-siliceous systems.[28] Previously, the applied atomic charges were calculated with split-valence basis sets which were indeed overestimated as compared to the other basis sets of this series. In order to determine the ratio between the charges of the oxygens of the Si–O–Al and Si–O–Si types, a simple analytical approximation, fitted with respect to R and ϑ for 79 crystallographically independent oxygens of all-siliceous zeolites[27–29] was applied to 63 oxygens of the Si–O–Al type within the five H-form zeolites.[30] The O charges of Si–O–Al type are higher by about 1.1 e with respect to those of Si–O–Si for similar internal coordinates (R, ϑ). Hence, we have adopted a model (called below the CRY model) based on the charge ratio 1.1 for all Si–O–Al oxygens and 1.0 for all Si–O–Si oxygens. Let us note that an alternative O charge distribution with more pronounced differences between charges,

i.e., charge ratio between 0.89 and 1.12 (called below the UDM model), was obtained by Uytterhoeven *et al.*[21]

For both CRY and UDM models, the charge values estimated on the basis of the electronegativity equalization method (EEM)[21] were used, which led to an ionicity of $q_0 = 6.584$ *e* for zeolite NaY. The usual O charges, obtained *via* PHF calculations performed with the STO-3G basis, range between −0.6 and −0.8 *e*, which leads to $q_0 = 4.8$ and 6.4 *e*. The ionicity $q_0 = 6.584$ *e* could thus be considered as a lower bound. As an upper estimate of q_0, we could consider values provided by PHF computations with a basis of 6-21G quality.[27] Then, O charges range between −1.1 and −1.2 *e* and q_0 is between 8.8 and 9.6 *e*, respectively. In this work, we will limit the q_0 range for zeolite Y to between 6.584 and 9.5 *e*.

IV. Co-adsorption

IV.1. Spatial models of the CO molecule

The determination of the molecular semi-axes of CO on the basis of a fitting procedure of the frequency of the experimentally observed two main bands of the fundamental vibrational transition of CO adsorbed in NaCaA has already been discussed.[19] The two peaks correspond to two different orientations of CO relative to the zeolite: Ca^{+2}–CO and Ca^{+2}–OC. In order to determine the three CO semi-axis values, the experimental IE obtained at small coverages is used as a third reference point. By the fitting procedure, we obtained four different models for CO, all corresponding to nearly the same molecular volume (*cf.* Table 7 in ref. 19). In this way, we have CO relevant parameters and IE expressions (eqn. (2)–(11) all given in ref. 19), which are needed to calculate the BS and IE values for NaRbY. The results are very close for all spatial CO models (Table 2). For this reason, in the following, we will consider the A model only which is in accordance with a conventional $r_\perp/r_\parallel \leq 1$ relation (with the exception of section IV.3).

We next calculated the IE and BS values for both CRY and UDM oxygen charge distribution models considering various q(Me) parameters (Me = Na, Rb) for both zeolites (Table 3). Compared to the experimental BS data,[16] the UDM model provides (by using a higher Me charge) rather underestimated BS values for NaY and overestimated ones for NaRbY or (by using a lower Me charge) underestimated BS values for both Y forms. As the BS values calculated with the CRY model are in agreement with the experimental ones (Table 3), it will be the only model used below.

IV.2. Interaction energy calculation

Using the CRY model, we then calculated the energy profiles along different directions passing through the center of a sodalite cage (Fig. 1, $R = 0$ corresponding to the center of the cage). The deepest Na^+–CO IE minimum was found near the Na_{II} ion in NaY (Fig. 1 and 2(a)) at $R = 21\ a_0$ (11.1 Å) or near the Rb_{II} ion at $R = 17\ a_0$ (Fig. 2(b)) in NaRbY. Both these sites were thus considered as the favoured positions for CO. One should mention that the dispersive IE component is very important for both cases (Fig. 2(a) and(b)). The situation inside NaRbY differs because of a higher contribution from the dispersive component. The position of CO with respect to the frameworks is shown in Fig. 3.

The slope of the IE terms with the probe internuclear ρ distance (Fig. 4) does not correspond to the absolute IE values usually estimated at equilibrium ρ_e (as in Fig. 2(a) and (b)). It is clear that for both Me = Na or Rb the "dipole" BS contribution largely dominates (Table 4) over the others in accordance with all previous estimations[1,4] (Fig. 4(a) and (b)). This explains why the simple electrostatic model proposed in ref. 7 was able to reproduce the experimental BS of CO adsorbed within the ZSM-5 and MOR frameworks.

An important point of our study is the charge dependences of the other atomic properties such as the polarizability and radius of the framework atoms (Table 1). In order to illustrate the influence of the variations of the Rb radius (2.48 Å)[23] on the BS calculations, we replaced the value 2.48 Å of Rb by 2.28 and 2.68 Å using the NaRbY model with $q(\mathrm{Rb}) = 0.65$ *e* and $q_0 = 9.5$ *e* and the SK intercombination rule. These replacements shift the BS from 12.9 cm^{-1} to 13.6 and 11.7 cm^{-1}, respectively, to be compared to the experimental data of 14 cm^{-1}. A small decrease in the BS by 0.2 cm^{-1} was also obtained on replacing the radius of Rb^+, 1.52 Å,[24] by 1.48 Å[31] for the same zeolite model. This variation changes the final BS and IE values only very slightly. As we did not find polarizability data $\alpha(Rb^+)$ substantially different from those adopted here (in ref. 22, $\alpha(Rb^+) = 1.8$ Å^3), the influence of the $\alpha(Rb^+)$ variation was not considered.

IV.3. Approximation of the repulsive coefficients

The electrostatic repulsion is the main reason for the unstable O–CO linear orientation already discussed in the literature.[19,32] As a result, repulsive O–CO coefficients cannot be calculated from the equilibrium position condition of the probe molecule relative to the negative framework O ion. Still, the BS calculation requires an approximation of the repulsive coefficients within the interval where the vibrational probability distribution with respect to the internuclear CO distance ρ cannot be neglected. Such an approximation can be based on the dependence of the CO dipole moment upon its internuclear distance ρ variation. The sign of the moment changes at larger ρ values and this corresponds to the inversion of the C and O charges leading to stable O_{zeol}–CO configurations for the higher vibrational states of CO. On this basis, we propose to

Table 2 Influence of the molecular CO model (*cf.* Table 7 in ref. 19) on the total interaction energy U_{tot} ($1 \times 10^{-3}\ E_h = 2.627$ kJ mol^{-1}) and band shift $\Delta\nu$ values while adsorbed within the NaRbY zeolite, with $q(\mathrm{Al})/q(\mathrm{Si}) = 0.8447$,[21] using parameters q(Rb) (*e*) and q_0 (*e*), corresponding to the CRY and UDM models of oxygen charge distribution

			CRY		UDM	
CO model	q(Rb)	q_0	$\Delta\nu$/cm^{-1}	$U_{tot}/10^{-3}\ E_h$	$\Delta\nu$/cm^{-1}	$U_{tot}/10^{-3}\ E_h$
A	1.0	9.5	25.7	−14.415	18.8	−9.170
	1.0	8.5	25.1	−14.712	20.0	−11.153
	0.9	9.5	19.5	−13.270	13.9	−9.193
C	1.0	9.5	20.3	−14.187	20.3	−10.278
	1.0	8.5	26.3	−14.433	20.5	−10.420
	0.9	9.5	20.9	−13.618	13.9	−9.709
D	1.0	9.5	26.4	−14.155	20.6	−10.463
	1.0	8.5	26.4	−14.390	20.7	−10.639
	0.9	9.5	20.8	−13.663	13.9	−9.951

Table 3 Total interaction energy U_{tot} (1×10^{-3} E_h = 2.627 kJ mol^{-1}) and band shift $\Delta\nu$ values of CO adsorbed within different NaY (Me = Na) and NaRbY (Me = Rb) zeolites, with q(Al)/q(Si) = 0.8447,[21] using parameters q(Me) (e) and q_0 (e), corresponding to the UDM and CRY oxygen charge distribution models. The CO molecular spatial parameters correspond to the A model (*cf.* Table 7 in ref. 19)

			NaY		NaRbY	
Model	q(Me)	q_0	$\Delta\nu$/cm^{-1}	$U_{tot}/10^{-3}$ E_h	$\Delta\nu$/cm^{-1}	$U_{tot}/10^{-3}$ E_h
UDM	1.0	9.5	24.7	−13.410	18.8	−9.170
	1.0	8.5	23.5	−12.598	20.0	−11.153
	0.9	9.5	20.0	−11.186	13.9	−9.193
	0.8	9.5	15.3	−10.623	9.8	−9.756
	0.7	9.5	12.3	−8.471	6.9	−8.811
CRY	1.0	9.5	34.0	−17.447	25.7	−14.415
	1.0	8.5	33.3	−17.417	25.1	−14.712
	0.9	9.5	30.1	−16.233	19.5	−13.270
	0.8	9.5	28.3	−15.038	15.1	−12.752
	0.7	9.5	22.7	−12.626	11.2	−11.502
Experiment[a]			29.0		14.0	

[a] Experimental $\Delta\nu$ value from ref. 16.

extend the coefficient evaluated at larger ρ values to shorter ρ ones. Within the $\rho \leq \rho_e$ interval, two different effective estimations of the repulsive coefficients dependence on ρ were used: the first (a) obtained by neglecting completely the repulsion term between CO and the framework oxygens (hereafter named "zero" approximation) and the second (b) by using a "dispersive" approximation, where the ρ dependence on the repulsive coefficient corresponds to the variation with ρ of the dispersive IE contribution.[19]

Neglect of the O–CO repulsion component could generate an error in the respective IE and BS values within the ρ interval where this repulsive interaction is valid. We indeed observed a fault of the "zero" approximation when omitting all repulsion terms between the framework oxygens and CO at the shorter ρ distances. For example, the most stable position for spatial model D (*cf.* Table 7 in ref. 19) within NaRbY corresponds to 6.49, 7.80, and 8.01 a_0 (3.43, 4.13, and 4.24 Å, respectively) from the O atoms and to 6.50 and 8.87 a_0 (3.47 and 4.69 Å, respectively) from the Si atoms resulting in IE values of -13.1×10^{-3} E_h (1×10^{-3} E_h = 2.627 kJ mol^{-1}), *i.e.*, of the same IE order as for the NaY case, and in a very large BS of 65 cm^{-1}. Applying now the dispersive approximation along the same direction, we obtain that the minimum is near Na_{II} (separated by 6.73 a_0) and near the O atoms of the 6-mem-

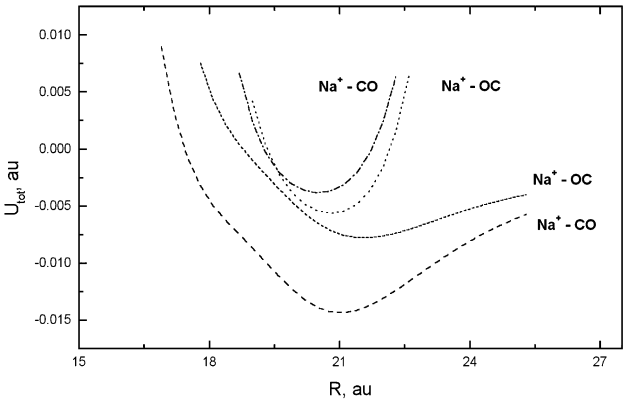

Fig. 1 Radial dependence (R = 0 corresponding to the center of the sodalite cage, a_0 = = 0.5292×10^{-10} m) of the interaction energy U_{tot} (1×10^{-3} E_h = 2.627 kJ mol^{-1}) between CO and zeolite NaY (q_0 = 9.5 e, q(Na) = 0.8 e, CRY oxygen charge distribution) along the C_3 axis passing through the hexagonal prism: dotted-dashed line for Na^+–CO, dotted for Na^+–OC; along the direction to the deepest minimum near Na^+: long-dashed line for Na^+–CO, short-dashed for Na^+–OC.

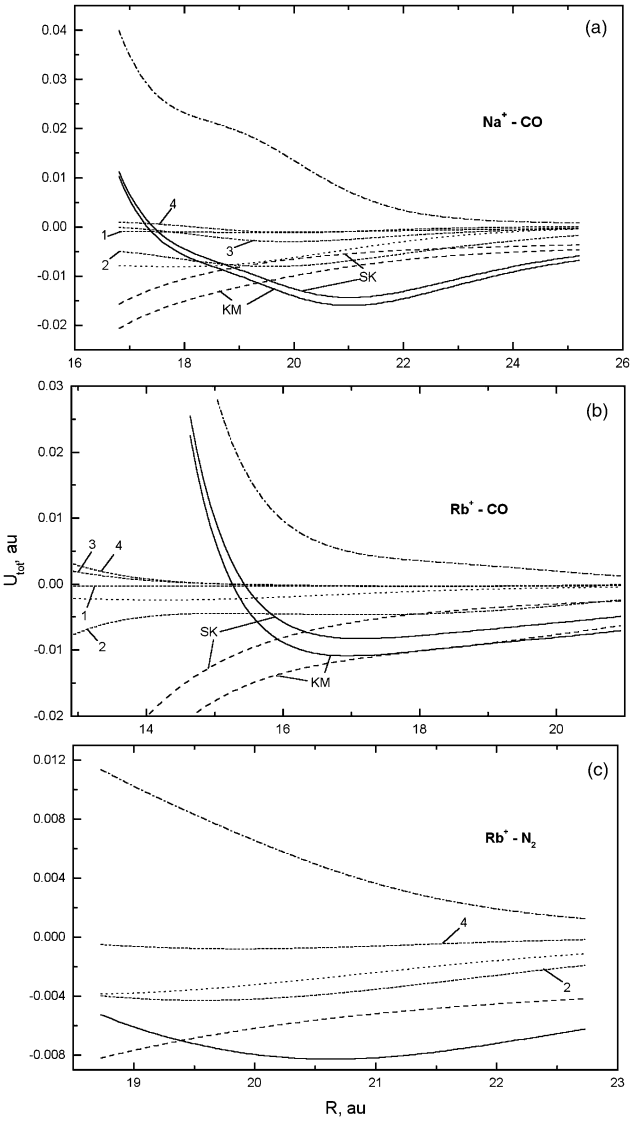

Fig. 2 Radial dependence (R = 0 corresponding to the center of the sodalite cage, $a_0 = 0.5292 \times 10^{-10}$ m) of the components of the interaction energy U_{tot} (1×10^{-3} E_h = 2.627 kJ mol^{-1}) between: (a) CO and zeolite NaY (Na–CO geometry, q_0 = 9.5 e, q(Na) = 0.8 e, CRY oxygen charge distribution); (b) CO and zeolite NaRbY (Rb–CO geometry, q_0 = 9.5 e, q(Rb) = 0.65 e, CRY oxygen charge distribution); (c) N_2 and zeolite NaRbY (q_0 = 9.5 e, q(Rb) = 0.65 e, CRY oxygen charge distribution). Full line U_i, long-dashed line U_{disp}, short-dashed line U^L_{el} (L is the order of the respective molecular multipole moment, given near each line), dotted U_{ind}, dotted-dashed U_{rep}.

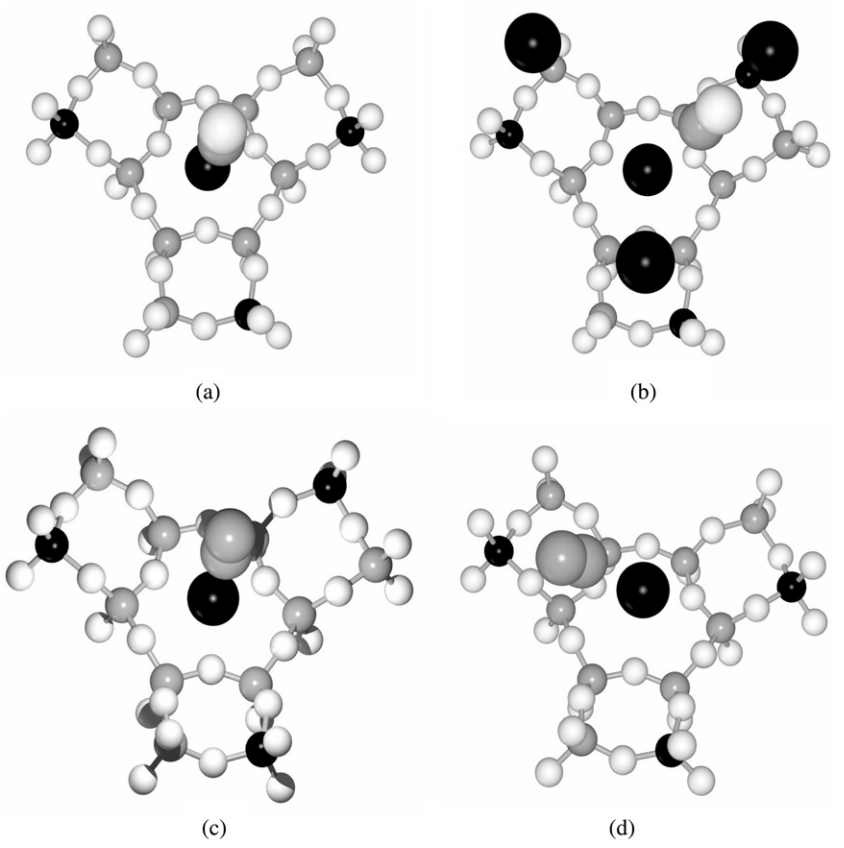

Fig. 3 Favoured positions of the CO (a), (b) and N_2 (c), (d) molecules with respect to the closest framework atoms of the NaY (a), (c) and NaRbY (b), (d) zeolite forms. The nearest Rb cations are shown in (b) only.

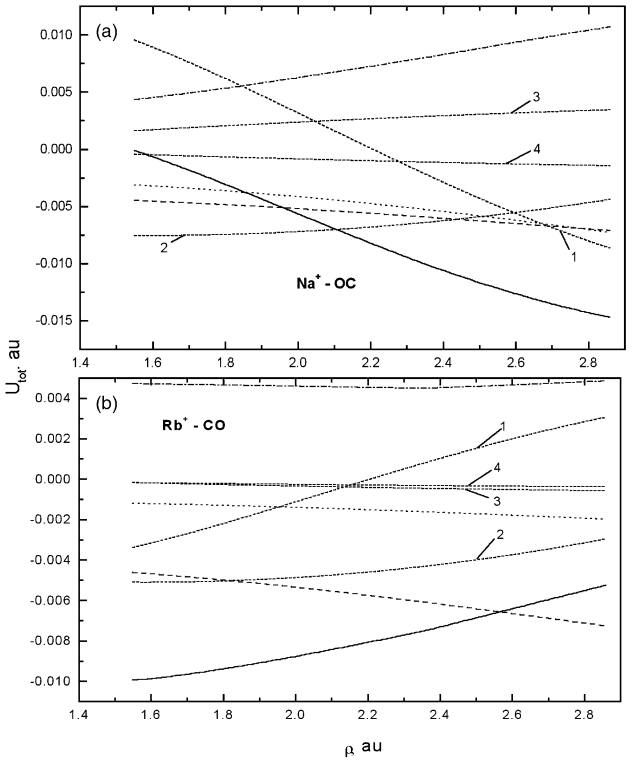

Fig. 4 Internuclear distance ρ dependence ($a_0 = 0.5292 \times 10^{-10}$ m) of the components of the interaction energy U_i between: (a) CO and zeolite NaY (Na–OC geometry, $q_0 = 9.5$ *e*, q(Na) = 0.8 *e*, CRY oxygen charge distribution); (b) CO and zeolite NaRbY (Rb–CO geometry, $q_0 = 9.5$ *e*, q(Rb) = 0.65 *e*, CRY oxygen charge distribution). Line notations as in Fig. 2.

bered ring (distances between 10.28 and 11.22 a_0) while the IE has a reasonable value of -8.236×10^{-3} E_h and the BS is 7 cm^{-1}. The dispersive approach considering the repulsive interactions with the closest O atoms thus helps to minimise the error in the determination of the favoured location of the probe molecule.

IV.4. Probe molecule location

Comparison between the X–CO distances (X = Na and closest oxygens O_i) in NaY (Table 5) shows a situation which could be well represented by the isolated Na–CO pair model (Fig. 3(a)). The situation is different for NaRbY where the Rb–CO and O_i–CO distances (O_i = closest oxygens, $i = 1, 2, 7, 8$) differ by 0.6 a_0 only, while for NaY this difference is about 2.3 a_0.

In order to verify the reason for the differences between NaRbY and NaY, we varied the contribution of the dispersive part to the total IE. The results are as follows: when replacing the KM intercombimation rule (eqn. (2)) by the SK rule, the dispersive IE decreases and the favoured geometry changes. CO moves towards the axis passing through the center of the 6-membered ring and the Rb_{II} cation. This is clearly seen by comparing the X–CO distances (Table 5). With the SK model, the minimal difference between Rb–CO and O_2–CO is a_0. Hence, replacement of the intercombination rule confirms the closer location of CO to the O atoms in NaRbY as compared to NaY.

To complete the picture, we should also mention the strong dependence of the IE upon the intercombination rule (eqn. (2)). The IE for CO in NaY zeolite is -15.99×10^{-3} E_h with KM and -12.68×10^{-3} E_h with SK. These values are higher and lower than the binding energy of the Na^+–CO pair, -14.65×10^{-3} E_h obtained at the *ab initio* QSID(T) level.[4] Furthermore, all theoretical results are higher than the reported experimental data, all contained in the -8.75×10^{-3}

Table 4 Comparison of the band shift $\Delta\nu$ components (*cf.* eqn. (15) in ref. 19) with $V = V_0 + U_i$ for CO (model A) adsorbed within zeolites NaY (q(Na) = 0.8 e, q_0 = 9.5 e, KM rule) and NaRbY (q(Rb) = 0.65 e, q_0 = 9.5 e, SK rule) using the CRY oxygen charge distribution

	$\Delta\nu$/cm^{-1}	
Component of IE	NaY	NaRbY
Dipole	50.3	17.9
Quadrupole	10.9	7.3
Octupole	−4.4	−0.7
Hexadecapole	−2.3	−1.0
Inductive	−12.8	−2.4
Dispersive	−11.4[a]	−7.8
Repulsive	−2.9[b]	−0.6
Total	30.0	12.9
Experiment[c]	29.0	14.0

[a] −7.9 cm^{-1} with the SK rule. [b] −4.2 cm^{-1} with the SK rule. [c] Ref. 16.

to -9.52×10^{-3} E_h interval.[33–35] For a correct comparison with experiment, our IE estimations could most probably be lowered after averaging over all available surface sites within the zeolite but this would require an additional statistical model not derived herein. However, it seems that the experimental data[33–35] are rather underestimated because they are lower than the heat of adsorption of N_2 in the NaZSM-5 and NaMOR forms (see Section V). Usually, this value for N_2 is smaller than for CO in a similar type of adsorbent.

In the IR spectra of CO in NaY and NaRbY reported in Fig. 2 of ref. 16, besides the dominant high frequency band, *i.e.*, BS values of 29 and 14 cm^{-1}, respectively, already extensively discussed and attributed to Me^+–CO (carbon down) adducts, two minor features are also present: a shoulder at 2138 cm^{-1} (BS = −5 cm^{-1}) and a lower frequency (LF) band appearing at 2122 cm^{-1} (BS = −21 cm^{-1}) for NaY and at 2126 cm^{-1} (BS = −17 cm^{-1}) for NaRbY. As far as the 2138 cm^{-1} band is concerned, its attribution is trivial. In fact the independence of the peak position *versus* the CO coverage, together with the observation of the same band for pure siliceous (cation free) silicalite,[36] confirms the assignment of this band to the "liquid-like" CO.[16,36–39] To our understanding, the latter should simply correspond to probe molecules adsorbed in the framework with the cationic sites already occupied by other preadsorbed CO molecules. The experimental evidence for the LF band is much more interesting and has stimulated the study of a possible Me^+–OC (oxygen-down) adduct. It is in fact worth noticing that the appearance of a minor LF band in the 2130–2110 cm^{-1} range (BS from −13 to −33 cm^{-1}) in the spectra of adsorbed CO is not peculiar to the faujasite forms (both X and Y);[3,16,40] it has also been observed for several other zeolites.[3,37–43] The fact that a very similar spectroscopic feature is observed in all zeolite forms means that such IR bands must have a common origin, probably an O-down adduct. Computationally, it has been reported that the O-down orientation of CO is stable within NaCaA.[19] In the present work, we obtained a stable orientation Me^+–OC for both cationic Y forms, characterized by BS values of −40.5 and −14.6 cm^{-1}, for NaY and NaRbY models corresponding to the cationic charges of 0.8 and 0.65 e (with SK rule in Table 5), respectively, and with IE values of −7.501 and -7.158×10^{-3} E_h smaller than those for the Me^+–CO configuration, *i.e.*, −14.410 and -8.283×10^{-3} E_h, respectively. We can therefore assert that we have both experimental and computational evidence for the stable oxygen-down Me^+–OC adducts in NaY and NaRbY since computed BS values are in qualitative agreement with the experimental ones (BS = −21 and −17 cm^{-1}, respectively). Furthermore, it is worth noting that the energetic barrier here computed for Na^+–CO ↔ Na^+–OC in NaY is in qualitative agreement only with the experimental result of 1.45×10^{-3} E_h in NaZSM-5.[43]

Finally, in order to further assign the BS in the IR spectra of adsorbed N_2, we needed a zeolite Y model which led to a good agreement with the experimental BS values of CO. Namely, sufficiently precise cation charges needed to be determined (Table 5). The variation of the Rb charge from 0.75 to 0.7 e was considered to take into account a more pronounced BS variation for the NaRbY form, *i.e.*, from 13.6 to 17.3 cm^{-1}, when varying the intercombination rule from KM to SK and conserving the Rb charge of 0.75 e (Table 6). This decrease in Rb charge allows us to hold the BS within ±1.3 cm^{-1} for the models obtained using the SK rule. Thus the models are of the same quality as those obtained with the KM rule, within ±1.0 cm^{-1}. Evidently, the real precision of our calculation is cruder than ±1.0 cm^{-1}, so that this step is a rather formal one and we did not try to reach a higher precision in the determination of the zeolite parameters (ionicity, charges). The chosen Na and Rb charges are denoted by an asterisk in Table 5.

V. N_2 adsorption

Nitrogen is also often used as a probe molecule[44–47] for zeolite studies. Its convenience comes from well known molecular parameters whose theoretical values (*cf.* Tables 1 and 2 in ref. 19) are in agreement with experimental ones. Different spatial N_2 models could be analyzed with respect to the anisotropy $\Delta_\perp^\parallel$ and vdW radius r_m, *e.g.*, which could be obtained from the third-order equation:

$$r_\perp{}^3 + a\rho_e \Delta_\perp^\parallel r_\perp{}^2 - (r_m/2)^3 = 0 \qquad (3)$$

where $r_\perp$ and $r_\parallel$ are the molecular semi-axes, $\Delta_\perp^\parallel = (r_\parallel - r_\perp)/\rho_e$

Table 5 Influence of the intercombination rule (eqn. (2)) on the band shift $\Delta\nu$, total interaction energy U_{tot} (1×10^{-3} E_h = 2.627 kJ mol^{-1}), electrostatic field T (E_h/ea_0 = 1 au = 5.1423×10^{11} V m^{-1}), and distances R_X ($a_0 = 0.5292 \times 10^{-10}$ m) between CO and the framework atoms X = O_i or Me_{II} for the MeY zeolite model (Me = Na or Rb) with ionicity q_0 = 9.5 e with/without nearest atom Me_{II} (the latter value given after the slash). The four final models chosen to calculate the $\Delta\nu$ and U_{tot} values for adsorbed N_2 are marked by an asterisk. The CO molecular spatial parameters correspond to the A model (*cf.* Table 7 in ref. 19)

Case	Me	q(Me)	$\Delta\nu$/cm^{-1}	$U_{tot}/10^{-3}$ E_h	$T/10^{-2}$ E_h/ea_0	R_{Me}/a_0	Distance to nearest O atoms R_{Oi}/a_0
KM	Na	0.80*	28.0	−15.992/−5.723	2.423/0.628	5.88	8.19(O_4), 8.37(O_7), 8.43(O_4), 8.45(O_7), 8.49(O_4), 8.74(O_7)
	Rb	0.75*	13.6	−12.038/−5.223	1.903/1.263	7.30	7.87(O_2), 8.04(O_8), 8.74(O_1), 8.80(O_7)
SK	Na	0.70	26.8	−12.679/−4.766	2.105/0.540	5.98	8.22(O_4), 8.30(O_7), 8.46(O_4), 8.60(O_7), 8.69(O_4), 8.89(O_7)
		0.75	27.4	−12.284	–	–	–
		0.80*	30.1	−14.410/−4.756	–	5.88	8.19(O_4), 8.37(O_7), 8.43(O_4), 8.45(O_7), 8.49(O_4), 8.74(O_7)
	Rb	0.65	12.9	−8.283	–	–	–
		0.70*	15.3	−8.681/−4.859	1.771/1.181	7.09	8.06(O_2), 8.20(O_8), 8.32(O_1), 8.64(O_8)
		0.75	17.3	−9.302	–	–	–

Table 6 Influence of the ionicity q_0 (e) and intercombination rule (eqn. (2)) on the total interaction energy U_{tot} (1×10^{-3} $E_h = 2.627$ kJ mol^{-1}) and band shift $\Delta\nu$ values of CO adsorbed within NaY (q(Na) = 0.8 e) and NaRbY (q(Rb) = 0.75 e) using the models shown in Table 5. The CO molecular spatial parameters correspond to the A model (*cf.* Table 7 in ref. 19)

		NaY		NaRbY	
q_0	Case	$\Delta\nu$/cm^{-1}	$U_{tot}/10^{-3}$ E_h	$\Delta\nu$/cm^{-1}	$U_{tot}/10^{-3}$ E_h
6.584	KM	24.9	−15.185	12.0	−13.207
	SK	27.2	−13.426	14.8	−9.256
8.5	KM	26.4	−15.734	12.6	−12.450
	SK	29.0	−14.083	14.5	−8.902
9.5	KM	28.0	−15.992	13.6	−12.038
	SK	30.1	−14.410	17.3	−9.302
Experiment[a]		29.0		14.0	

[a] Ref. 16.

is a dimensionless parameter, ρ_e being the equilibrium N_2 internuclear distance, and $a = 1$ or $3/2$ for the ellipsoid or spherocylinder type volume, respectively. This equation is the consequence of the condition we imposed in order that the ellipsoid or spherocylinder model would correspond to a sphere of vdW radius r_m of the same volume.

We did not repeat here the optimizations of the molecular sizes of N_2, as developed for CO, principally owing to the unreliable small BS of adsorbed N_2 as compared, for example, to the value of the three-body interaction dispersive terms disregarded in this paper (5 cm^{-1} for the N_2/NaA zeolite system).[48] We chose to study eight different spatial models for N_2, using the same zeolite models which provided a reasonable agreement between the theoretical and experimental BS for CO (Table 7). Having no precise data about the anisotropy $\Delta^{\parallel}_{\perp}$, we considered a series of N_2 models whose $\Delta^{\parallel}_{\perp}$ values range between 0 and 0.45 and $r_m = 4.26$ Å.[49] As presented in Table 8, all models lead to lower BS for NaRbY than for NaY. The differences $\Delta\nu$(NaY) − $\Delta\nu$(NaRbY) are usually lower than the experimental value,[16] *i.e.*, 8 cm^{-1}.

The configuration of the Me^+–N_2 pair is almost linear within both Y forms studied here, *i.e.*, the angle varies around 178° for Na^+–N_2 (Fig. 3(c)) and 174° for Rb^+–N_2 (Fig. 3(d)). As a result, the behaviour of the IE and BS with $\Delta^{\parallel}_{\perp}$ and r_m is determined by an increase in the parallel semi-axis and in the Me^+–N_2 intermolecular distance at the favoured location. Higher Me^+–N_2 distances lead to a decrease in all IE components (in absolute value). The dispersive interaction (together with the inductive one) is the source of the negative contribution to the BS *via* an increase in molecular polarizability with the vibrational excitation, while the positive BS component comes either from a decrease in the electrostatic IE or from an increase in the repulsive IE (Table 9). The resulting total BS increase with $\Delta^{\parallel}_{\perp}$ noted in Table 9 comes from a relative increase in the repulsive BS contribution and from a decrease (in absolute value) of the inductive one. Finally, a qualitative coincidence between the calculated and experimental BS is observed with the anisotropy $\Delta^{\parallel}_{\perp} = 0.35$, *i.e.*, 1.3 and −4.3 cm^{-1} with the KM rule, or 2.5 and −1.9 cm^{-1} with the SK rule for NaY and NaRbY, respectively, as compared to the experimental data of 4 and −4 cm^{-1} for both Y forms, respectively. A nice correlation with the experimental BS is observed with $\Delta^{\parallel}_{\perp} = 0.45$ (Table 9). Comparing this interval with the 0.25 found theoretically for molecular hydrogen,[52] one may think that the interval 0.35–0.45 is not too exaggerated.

Table 7 N_2 molecular spatial models

Type[a]	$\Delta^{\parallel}_{\perp}$	$r_{\parallel}$/Å	$r_{\perp}$/Å	r_m[a]/Å
A	0.05	2.158	2.103	4.26
B	0.15	2.216	2.051	4.26
C	0.25	2.276	2.001	4.26
D	0.35	2.339	1.954	4.26
E	0.45	2.404	1.909	4.26
F	0.55	2.471	1.867	4.26
G	0.45	2.320	1.825	4.09
H	0.45	2.419	1.924	4.29
Experiment				4.26[b], 4.13[c], 4.09[d]

[a] Perpendicular $r_{\perp}$ and parallel $r_{\parallel}$ radius were calculated using the condition between an equivalent volume of sphere of vdW radius r_m and a spherocylinder with $r_{\perp}$ and $r_{\parallel}$ semi-axes, *e.g.*, *via* eqn. (3). [b] Ref. 49. [c] Ref. 50. [d] Ref. 51.

In order to analyse the behaviour of the IE as a function of the vdW radius r_m, we varied r_m between the lower known experimental value 4.09 Å and the upper limit 4.29 Å obtained from the BS fitting procedure for CO (*cf.* Table 7 in ref. 19), whose molecular sizes are very close to those of N_2. The anisotropy $\Delta^{\parallel}_{\perp} = 0.45$ for N_2 shows a relatively good coincidence between the theoretical and experimental BS for both Y forms (Table 9 with ionicity $q_0 = 9.5$ e). An increase in r_m and, consequently, in the parallel semi-axis results in a decrease in the IE and an increase in the BS (Table 9), while at smaller r_m we observe a minimum IE with a dominant dispersive component and underestimated BS values.

Analysis of the interaction between N_2 and both Y forms allows us to propose several major distinctions between the NaY and NaRbY systems. They are summarised in Table 10. The favoured position for N_2 is close to Na_{II} for both vdW coefficient estimations, SK and KM, while with Rb_{II}, N_2 is closer to two O framework atoms using the KM rule, and to one O with SK. This last difference regarding the number of closest oxygens can be easily explained due to the higher dispersive interactions estimated with the KM rule. Detailed results obtained for a lower ionicity, *i.e.*, $q_0 = 6.584$ e[21] (not discussed here), do not provide a better agreement with the experimental BS (Table 7), but the principal features in the geometry and BS relation for both Y forms are similar.

Unfortunately, we do not have any data on the heat of adsorption of N_2 within both Y forms so we can only compare the order of values. The overestimated dispersive IE usually addressed to the KM intercombination rule may be compared with available data for the isosteric heat of adsorption for N_2 in the Na (-10.62×10^{-3} E_h, 1×10^{-3} $E_h = 2.627$ kJ mol^{-1}) and Rb (-8.22×10^{-3} E_h) forms of ZSM-5.[45] The first value is not far from the -11.42×10^{-3} E_h obtained for Na mordenite.[46] For both NaY and NaRbY, the KM rule leads to IE values of −10.47 and -7.38×10^{-3} E_h, respectively, which correlate well with the upper given values. Evidently, any data available for the heat of adsorption within both forms could strongly limit the set of appropriate N_2 models.

Summarising this section, we conclude that the simultaneous comparison of the BS of both different CO and N_2 probe molecules allows us to define a narrower range for the ionicity q_0 value, because a qualitative coincidence with the experimental BS for N_2 can be reached, for comparison, with $q_0 = 8.5$–9.5 e.

VI. Electrostatic field calculation

The zeolite fragment consisting of 19 or more cells as explained above (see section III) allows us to estimate the electrostatic field created by the whole framework. We computed the field values at the CO (Table 5) and N_2 (Table 10) favoured locations within both forms. Our estimations range between 2.4 and 2.1×10^{-2} E_h/ea_0 (1×10^{-2} $E_h/ea_0 = 5.1423$ V nm^{-1}) for NaY and between 1.9×10^{-2} and 1.6×10^{-2} E_h/ea_0 for NaRbY. These field values for these Y forms are higher than

Table 8 Total interaction energy U_{tot} (1×10^{-3} E_h = 2.627 kJ mol^{-1}) and band shift $\Delta\nu$ values of N_2 molecule adsorbed within different NaY (Me = Na) and NaRbY (Me = Rb) zeolites with $q(Al)/q(Si) = 0.8447$[21] using alkali-metal charge q(Me) (e), ionicity q_0 (e), and CRY oxygen charge distribution. The N_2 molecular spatial parameters are presented in Table 7

			KM		SK	
q_0	q(Me)	$\Delta_\perp^\parallel$	$\Delta\nu$/cm^{-1}	$U_{tot}/10^{-3}$ E_h	$\Delta\nu$/cm^{-1}	$U_{tot}/10^{-3}$ E_h
Zeolite NaY[a]						
9.5	0.8	0.05	−2.1	−11.365	−0.7	−9.926
		0.15	−0.5	−10.965	0.7	−9.583
		0.25	0.4	−10.470	1.7	−9.170
		0.35	1.3	−9.933	2.5	−8.710
		0.45	2.6	−9.397	4.0	−8.247
		0.45[b]	−0.9	−12.466	0.4	−10.883
		0.45[c]	2.8	−9.253	4.1	−8.119
		0.55	3.4	−8.886	4.8	−7.798
8.5	0.8	0.05	1.6	−11.403	2.9	−9.886
		0.15	2.6	−10.931	3.6	−9.501
		0.45	6.8	−9.676	8.4	−8.413
6.584	0.8	0.05	−7.5	−11.393	−5.4	−9.807
		0.35	−6.0	−10.084	−3.9	−8.141
Zeolite NaRbY [d]						
9.5	0.75[e]	0.35	−4.3	−8.120	−1.9	−5.140
		0.45	−3.3	−8.026	−1.1	−5.075
		0.55	−2.6	−7.892	−0.1	−5.573
8.5	0.75[e]	0.05	−3.8	−8.820	−0.5	−6.138
		0.15	−2.6	−8.630	0.0	−6.090
		0.35	−2.2	−8.213	0.1	−5.888
		0.45	−1.4	−8.106	0.6	−5.869
6.584	0.75[e]	0.15	−8.4	−8.906	−4.8	−5.056
		0.45	−8.6	−8.579	−5.3	−5.832

[a] Experimental $\Delta\nu$ value[16] is 4 cm^{-1}. [b] r_m = 4.09 instead of 4.26 Å in other cases. [c] r_m = 4.29 instead of 4.26 Å in other cases. [d] Experimental $\Delta\nu$ values[16] are 4 and −4 cm^{-1}, the first value being related to the Na_{II} ions remaining after ion exchange in accordance with the conclusions of ref. 16. [e] *0.7 e for SK case.*

the known experimental data, *i.e.*, 0.99×10^{-2} and 0.47×10^{-2} E_h/ea_0 for NaY and NaRbY,[16] respectively, 1.18×10^{-2} and 0.53×10^{-2} E_h/ea_0 for NaMOR and RbMOR,[46] 1.22×10^{-2}, 0.64×10^{-2} E_h/ea_0 for NaZSM-5 and RbZSM-5.[45] This difference between the real and modelled field values can be mainly associated with the neglect of the high order multipole moments (higher than the charges) of the zeolite atoms as was observed while simulating the electrostatic field over TiO_2[53] or within different sieves.[30,54] Electrostatic potential can be overestimated up to 80–100% for both the H-form aluminosilicates[30] and aluminophosphates (Al/P = 1).[54,55]

In order to compare, for both Y forms, the importance of the closest cation to the adsorbed molecule, we calculated the field experienced by CO and N_2 with and without the closest ion at position II. For NaY, the field values are 2.348×10^{-2} and 0.730×10^{-2} E_h/ea_0 with and without Na (Table 10), respectively, at the N_2 favoured location. The latter ratio clearly emphasizes the role of the Na cation in comparison to the analogous field variations in the absence of Rb_{II} in NaRbY, namely 1.692×10^{-2} and 0.983×10^{-2} E_h/ea_0. The rotation of the total electrostatic field vector obtained at the CO favoured position with/without alkali-metal cation can illustrate the situation: the vector turns by 113° for Na and by 52° for Rb, considering the SK rule.

These field variations support the idea, already mentioned in section III, that the adsorption within NaY is governed by the Na ion, due mainly to its high contribution to the field as compared to an essentially lower field created by the Rb ion at the CO or N_2 favoured positions.

Table 9 Comparison of the band shift $\Delta\nu$ components (*cf.* eqn. (15) in ref. 19) with $V = V_0 + U_i$ for different N_2 models ($\Delta_\perp^\parallel$ = 0.05 and 0.45, r_m = 4.26 Å) adsorbed in zeolite NaY using q(Na) = 0.8 e, q_0 = 9.5 e, SK rule (eqn. (2))

	$\Delta\nu$/cm^{-1}	
IE component	$\Delta_\perp^\parallel$ = 0.05	$\Delta_\perp^\parallel$ = 0.45
Quadrupole	6.0	4.9
Hexadecapole	1.1	0.5
Inductive	−9.2	−6.6
Dispersive	−6.2	−5.6
Repulsive	7.7	10.3
Total	−0.7	4.0

VII. Conclusions

In this work, we have considered CO and N_2 probe molecules adsorbed within NaY and NaRbY zeolites. The CO spatial parameters were taken from a preliminary fitting procedure relative to the adsorption over another zeolite, *i.e.*, Na_4Ca_4A,[19] while N_2 parameters were varied to keep the van der Waals radius close to the experimental value. Central multipole moments and polarizabilities of the probe molecules together with their internuclear distance dependences were validated considering their IE and BS calculations within the framework models.

Good quantitative agreement between the calculated and experimental BS, within ±1 cm^{-1},was achieved for CO. For N_2 the agreement is only qualitative. Both results were

Table 10 Influence of the intercombination rule (eqn. (2)) on the band shift $\Delta\nu$, total interaction energy U_{tot} (1×10^{-3} $E_h = 2.627$ kJ mol^{-1}), electrostatic field T ($E_h/ea_0 = 1$ au $= 5.1423 \times 10^{11}$ V m^{-1}), and distances R_X ($a_0 = 0.5292 \times 10^{-10}$ m) between N_2 (model C, Table 7) and the framework atoms X = O_i, Si or Me_{II} for the MeY zeolite model with ionicity $q_0 = 9.5$ e with/without nearest atom Me_{II} (the latter value given after the slash)

Case	Me	q(Me)	$\Delta\nu^a$/cm^{-1}	$U_{tot}/10^{-3}$ E_h	$T/10^{-2}$ E_h/ea_0	R_{Me}/a_0	R_X/a_0
KM	Na	0.80	0.4	−10.470/−4.681	2.348/0.730	6.17	7.74(O_7), 8.13(O_4), 8.31(O_4), 8.70(Si), 8.77(O_1), 8.90(Si)
	Rb	0.75	−4.4	−7.396/−3.769	1.692/0.983	7.91	7.70(O_7), 7.90(O_2), 8.36(O_1), 8.68(O_8), 8.90(Si), 9.22(Si)
SK	Na	0.80	1.7	−9.170/−3.829	2.337/0.728	6.19	7.76(O_7), 8.13(O_4), 8.34(O_4), 8.71(Si), 8.78(O_1), 8.92(Si)
	Rb[b]	0.70	−1.9	−5.140/−3.024	1.600/0.940	7.92	7.77(O_7), 8.06(O_2), 8.33(O_1), 8.86(O_8), 9.02(Si), 9.24(Si)

[a] Experimental $\Delta\nu$ values are 4 cm^{-1} for NaY and 4, −4 cm^{-1} for NaRbY, the first value for NaRbY being related to the Na_{II} ions remaining after ion exchange in accordance with the conclusions of ref. 16. [b] the D model of the N_2 molecule is used here instead of C in other cases, see Table 7.

obtained using an O charge distribution deduced from results of *ab initio* periodic Hartree–Fock computations. The best coincidence of the BS values was reached with very similar cationic charges for both zeolite forms. In such a way, we confirmed the applicability of the CO model in different zeolites of A and Y type presenting comparable atomic (ionic) characteristics.

The importance of the dispersive interaction term was clearly shown for both CO and N_2 favoured locations in the NaRbY form. The interaction of CO with a Rb_{II} cation of higher radius and lower electrostatic field than Na_{II}, could be accompanied by a partial CO coordination with the O atoms in one of the three nearest 4-membered rings. Then, the representation of the adsorbed probe using the isolated "cation–probe" pair only is clearly not valid in this case. The decrease in the dispersive interaction calculated *via* the intercombination Slater–Kirkwood rule confirms that the CO favoured location remains close to the O atoms within NaRbY. In the case of N_2, the dispersive interaction is clearly more important. N_2 is closer to the NaRbY framework oxygens than to Rb; such a configuration was obtained with any inter-combination rule applied herein.

One of the main results is that the present parametrisation of the CO model based on the BS values and one IE value is not sufficient to yield energy differences quantitatively for both the CO and OC orientations toward the zeolite. But this parametrisation of the CO model fitted for the NaCaA type zeolite[19] can satisfactorily produce correct BS values for both the CO and OC orientations in the Y framework. If the parametrisation were wrong then the errors should be different for the different A and Y frameworks with the different locations of the nearest oxygen atoms to the probe.

We thus demonstrated, on the one hand, that the spatial CO model fitted over the NaCaA zeolite form can be applied to other zeolites, *i.e.*, NaY and NaRbY and, on the other hand, that by replacing Na by a heavier cation such as Rb, the resulting location relative to the zeolite framework is essentially different owing to the increased dispersive interaction. Such a difference was noted earlier in the literature when spatial restrictions on the molecular motions were imposed by the respective size of the MOR zeolite,[45] which is not the case for large Y cavities.

Acknowledgement

The authors wish to thank the FUNDP for the use of the Namur Scientific Computing Facility (SCF) Center, a common project between the FNRS, IBM-Belgium, and FUNDP as well as Accelrys for the use of their data in the framework of the "Catalysis 2000" consortium. They are grateful for the partial support of the Interuniversity Research Program on Quantum Size Effects in Nanostructured Materials (PAI/IUAP 5/01) initiated by the Belgian Government.

References

1 J. Sauer, P. Ugliengo, E. Garrone and V. R. Saunders, *Chem. Rev.*, 1994, **94**, 2095.
2 K. Beck, H. Pfeifer and B. Staudte, *J. Chem. Soc., Faraday Trans.*, 1993, **89**, 3995.
3 S. Bordiga, E. Garrone, C. Lamberti, A. Zecchina, C. Otero Areán, V. B. Kazansky and L. M. Kustov, *J. Chem. Soc., Faraday Trans.*, 1994, **90**, 3367.
4 A. M. Ferrari, P. Ugliengo and E. Garrone, *J. Chem. Phys.*, 1996, **105**, 4129.
5 A. M. Ferrari, K. M. Neyman and N. Rösch, *J. Phys. Chem. B*, 1997, **101**, 9292.
6 A. M. Ferrari, K. M. Neyman, S. Huber, H. Knözinger and N. Rösch, *Langmuir*, 1998, **14**, 5559.
7 C. Lamberti, S. Bordiga, F. Geobaldo, A. Zecchina and C. Otero Areán, *J. Chem. Phys.*, 1995, **103**, 3158.
8 C. O. Veloso, J. L. F. Monteiro and E. F. Sousa-Aguiar, *Stud. Surf. Sci. Catal.*, 1994, **84**, 1913.
9 F. Bouchet, H. Fujisawa, M. Kato and T. Yamaguchi, *Stud. Surf. Sci. Catal.*, 1994, **84**, 2029.
10 A. Seidel and B. Boddenberg, *Z. Naturforsch. A.*, 1994, **50**, 199.
11 B. Boddenberg and T. Sprang, *J. Chem. Soc., Faraday Trans.*, 1995, **91**, 163.
12 T. Sprang and B. Boddenberg, *J. Chem. Soc., Faraday Trans.*, 1995, **91**, 555.
13 M. Hunger, G. Engelhardt and J. Weitkamp, *Microporous Mater.*, 1995, **3**, 497.
14 H. Klein, H. Fuess and M. Hunger, *J. Chem. Soc., Faraday Trans.*, 1995, **91**, 1813.
15 C. Lamberti, G. Spoto, D. Scarano, C. Paze, M. Salvalaggio, S. Bordiga, A. Zecchina, G. Turnes Palomino and F. D'Acapito, *Chem. Phys. Lett.*, 1997, **269**, 500.
16 G. L. Marra, A. N. Fitch, A. Zecchina, G. Ricchiardi, M. Salvalaggio, S. Bordiga and C. Lamberti, *J. Phys. Chem. B.*, 1997, **101**, 10 653.
17 D. M. Bishop, *Int. Rev. Phys. Chem.*, 1994, **13**, 21.
18 M. Fernandez-Garcia, J. C. Conesa and F. Illas, *Surf. Sci.*, 1996, **349**, 207.
19 A. V. Larin, L. Leherte and D. P. Vercauteren, *Phys. Chem. Chem. Phys.*, 2002, **4** , DOI: b107243a.
20 A. V. Larin and E. Cohen de Lara, *J. Chem. Phys.*, 1994, **101**, 8130.
21 L. Uytterhoeven, D. Dompas and W. J. Mortier, *J. Chem. Soc., Faraday Trans.*, 1992, **88**, 2753.
22 A. Dalgarno, *Adv. Chem. Phys.*, 1967, **12**, 143.
23 N. S. Akhmetov, *Inorganic Chemistry*, Vysshaya Schkola, Moscow, 1975.
24 R. D. Shannon, *Acta Crystallogr., Sect. A*, 1976, **32**, 751.
25 P. Broier, A. V. Kiselev, E. A. Lesnik and A. A. Lopatkin, *Z. Fiz. Khim.*, 1968, **42**, 2556.
26 J. G. Kirkwood, *Phys. Z.*, 1932, **33**, 57.
27 A. V. Larin, L. Leherte and D. P. Vercauteren, *Chem. Phys. Lett.*, 1998, **287**, 169.
28 A. V. Larin and D. P. Vercauteren, *Int. J. Quantum Chem.*, 1998, **70**, 993.
29 A. V. Larin and D. P. Vercauteren, *Int. J. Inorg. Mater.*, 1999, **1**, 201.
30 A. V. Larin and D. P. Vercauteren, *J. Mol. Catal. A*, 2001, **168**, 123.
31 L. Pauling, *The Nature of the Chemical Bond and the Structure of Molecules and Crystals*, Cornell University Press, 3rd edn., 1960, p. 518.

32 E. A. Colbourn and W. C. Mackrodt, *Surf. Sci.*, 1982, **117**, 571; E. A. Colbourn and W. C. Mackrodt, *Surf. Sci.*, 1984, **143**, 391.
33 T. A. Egerton and F. S. Stone, *Trans. Faraday Soc.*, 1970, **66**, 2364.
34 T. A. Egerton and F. S. Stone, *J. Colloid Interface Sci.*, 1972, **38**, 195.
35 T. A. Egerton and F. S. Stone, *J. Chem. Soc., Faraday Trans. 1*, 1973, **69**, 22.
36 A. Zecchina, S. Bordiga, G. Spoto, L. Marchese, G. Petrini, G. Leofanti and M. Padovan, *J. Phys. Chem.*, 1992, **96**, 4991.
37 S. Bordiga, E. Escalona Platero, C. Otero Areán, C. Lamberti and A. Zecchina, *J. Catal.*, 1992, **137**, 179.
38 A. Zecchina, S. Bordiga, C. Lamberti, G. Spoto, L. Carnelli and C. Otero Areán, *J. Phys. Chem.*, 1994, **98**, 9577.
39 S. Bordiga, C. Lamberti, F. Geobaldo, A. Zecchina, G. Turnes Palomino and C. Otero Areán, *Langmuir*, 1995, **11**, 527.
40 S. Bordiga, D. Scarano, G. Spoto, A. Zecchina, C. Lamberti and C. Otero Areán, *Vib. Spectrosc.*, 1993, **5**, 69.
41 H. Böse and H. Förster, *J. Mol. Struct.*, 1990, **218**, 393.
42 M. Katoh, T. Yamazaki and S. Ozawa, *Bull. Chem. Soc. Jpn.*, 1994, **67**, 1246.
43 C. Otero Areán, A. A. Tsyganenko, E. Escalona Platero, E. Garrone and A. Zecchina, *Angew. Chem. Int. Ed. Engl.*, 1998, **37**, 3161.
44 E. Cohen de Lara and Y. Delaval, *J. Chem. Soc., Faraday Trans. 2*, 1978, **74**, 790.
45 T. Yamazaki, I. Watanuki, S. Ozawa and Y. Ogino, *Bull. Chem. Soc. Jpn.*, 1988, **61**, 1039.
46 Y. Kuroda, Y. Yoshikawa, S.-I. Konno, H. Hamano, H. Maeda, R. Kumashiro and M. Nagao, *J. Phys. Chem.*, 1995, **99**, 10 621.
47 F. Geobaldo, C. Lamberti, G. Ricchiardi, S. Bordiga, A. Zecchina, G. Turnes Palomino and C. Otero Areán, *J. Phys. Chem.*, 1995, **99**, 11167.
48 H. Kono and A. Takasaka, *J. Phys. Chem.*, 1987, **91**, 4044.
49 E. R. Cohen and G. Birnbaum, *J. Chem. Phys.*, 1977, **66**, 2443.
50 I. R. Dagg, A. Anderson, S. Yan, W. Smith and L. A. A. Read, *Can. J. Phys.*, 1985, **63**, 625.
51 G. Birnbaum and E. R. Cohen, *Mol. Phys.*, 1976, **32**, 161.
52 W. Kolos and C. C. J. Roothaan, *Rev. Mod. Phys.*, 1960, **32**, 219.
53 P. Reinhardt, M. Causà, C. M. Marian and B. A. Heß, *Phys. Rev. B*, 1996, **54**, 14 812.
54 A. V. Larin and D. P. Vercauteren, *J. Mol. Catal. A*, 2001, **166**, 73.
55 A. V. Larin and D. P. Vercauteren, *Int. J. Quantum Chem.*, 2001, **83**, 70.